Extended Abstracts of the 2003 International Conference on Solid State Devices and Materials, Tokyo, 2003, pp. 448-449

P2-19L

Improved Modeling Technique for On-Chip Silicon Spiral Inductors

Ming-Hsiang Cho, Guo-Wei Huang, Kun-Ming Chen, Sheng-Yu Wen, and Sheng-Chun Wang

National Nano Device Laboratories
1001-1 Ta Hsueh RD., Hsinchu 300, Taiwan, R.O.C.
Phone: +886-3-5726100 E-mail: gwhuang@ndl.gov.tw

1. Introduction

Modeling work on spiral inductors is significant for commercial silicon radio frequency integrated circuits (RFICs). In this study, we develop an improved model which accounts for the skin effect [1],[2] of the metallic trace and the loss between the two terminals. A new extraction procedure for model parameters is also proposed. The automatic extraction program can generate the unique parameter set of circuit elements for the spiral inductor. Experimental results indicate that the proposed model can simulate the transmission behavior of inductor more accurately than the conventional 9-element model does.

2. Improved Equivalent-Circuit Model

The equivalent circuit diagram of the proposed model is illustrated in Fig. 1. The additional branch composed of R_{sk} and L_{sk} is adopted to characterize the frequency-dependent skin effect and the shunt R_p is introduced to interpret the effective loss between the two terminals. Therefore, the inductor can be modeled comprehensively.

3. Modeling Procedure and Extraction Algorithms

Metal Resistance and Inductance

High-frequency on-wafer measurements from 0.1 to 20 GHz were performed with an HP8510C Vector Network Analyzer. After de-embedding the corresponding OPEN dummy device by Y-parameter subtraction method, two-port S-parameters are converted to one-port Z-parameters (Z_{1port}) by grounding the other port. At low frequency, three initial conditions [3] can be expressed as

$$R_{dc} = \frac{R_s R_{sk}}{R_s + R_{sk}} \tag{1}$$

$$L_{dc} = L_s + \left(\frac{R_s}{R_s + R_{sk}}\right)^2 \cdot L_{sk} \tag{2}$$

$$\frac{L_s}{L_{sk}} = 0.315 \cdot \frac{R_{sk}}{R_s} \tag{3}$$

where R_{dc} and L_{dc} can be obtained from real part and imaginary part of Z_{1port} at the lowest frequency, respectively. The effective inductance as a function of frequency can be evaluated as $L = \mathrm{Im}(Z_{1port})/(2\pi f)$. As the frequency increases, the current in metal strip tends to shift to the conductor surface, thereby reducing the effective inductance. However, when the frequency goes higher, the effective inductance will rise owing to the metal-to-metal coupling of spiral inductor. Here we define the first local minimum value of L as L_s. Based on the above results, R_{sk}, R_s, and L_{sk} can be calculated from the following equations

$$a \cdot R_{sk}^3 - (a \cdot R_{dc}) \cdot R_{sk}^2 - R_{dc} = 0 \tag{4}$$

$$R_s = a \cdot R_{sk}^3 \tag{5}$$

$$L_{sk} = \frac{L_s R_s}{0.315 \cdot R_{sk}} \tag{6}$$

where a = $0.315 \cdot (L_{dc} - L_s)/(L_s R_{dc}^2)$. R_{sk} can be calculated as the positive root of eq. (4).

Metal-To-Metal Parasitics

At high-frequency regime, the impedance of the upper part of the proposed model in Fig.1 is only composed of R_s, L_s, C_p, and R_p and can be expressed as

$$Z_{up} = \frac{1}{-Y_{21}} = \frac{\left(\frac{1}{R_p} + \frac{R_s}{R_s^2 + \omega^2 L_s^2}\right) - j\left(\omega C_p - \frac{\omega L_s}{R_s^2 + \omega^2 L_s^2}\right)}{\left(\frac{1}{R_p} + \frac{R_s}{R_s^2 + \omega^2 L_s^2}\right)^2 + \left(\omega C_p - \frac{\omega L_s}{R_s^2 + \omega^2 L_s^2}\right)^2} \tag{7}$$

The self-resonance frequency of Z_{up} occurs when $(\omega_{sr}^2 L_s^2 C_p - L_s + C_p R_s^2) = 0$, and the value of C_p can be evaluated as $C_p = L_s/(R_s^2 + \omega_{sr}^2 L_s^2)$. The parameter R_p can be extracted at the frequency point where the maximum value of $\mathrm{Im}(Z_{up})$ occurs

$$R_p^2 \cdot (\mathrm{Im}(Z_{up}) \cdot (b^2 + c^2) - b) + \mathrm{Im}(Z_{up}) \cdot (2cR_p + 1) = 0 \tag{8}$$

where b = $\omega C_p - \omega L_s/(R_s^2 + \omega^2 L_s^2)$, c = $R_s/(R_s^2 + \omega^2 L_s^2)$, and R_p is the positive root of eq. (8).

Substrate Parasitics

The substrate parasitics can be mathematically derived [4] and extracted based on $C_{si} = L_s/(R_s^2 + \omega_{sr}^2 L_s^2) - C_p$ and $R_{si} = 1/(1/R_{max} + 1/R_p)$, where ω_{sr} is the self-resonance angular frequency of Z_{1port} and R_{max} is the maximum value of $\mathrm{Re}(Z_{1port})$. Figure 2 shows the flow chart of the modified extraction macro, and the calculation method of C_{ox} is illustrated in the last step.

4. Results and Discussion

To substantiate the proposed model, we compared the simulated data of conventional model and modified model with the measured data of a 4 turn 3.3 nH inductor with the dimensions of metal width (W) = 13μm , space (S) = 2μm , inner diameter (ID) = 146μm. Figure 3 shows that modeling results of the return loss and the insertion loss for the spiral inductor. It is obviously that the simulation results of transmission characteristics is improved based on the proposed model due to the addition of R_p, Figures 4 and 5 show the modeling results of inductance and quality factor (Q) of the inductor, respectively. The improvement of modeling results at low frequency is achieved by accounting for the frequency dependent skin effect which is presented by R_{sk} and L_{sk} in this study.

5. Conclusions

An improved modeling technique for planar spiral inductors is proposed in this study. The model parameters is SPICE-compatible and can be extracted efficiently and precisely with the modified extraction process. Compared with the traditional model, the proposed model can simulate the transmission characteristics of inductor accurately beyond the self-resonance frequency.

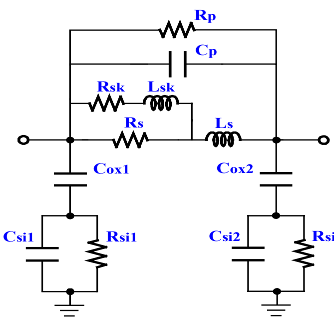

Fig. 1 Illustration of the proposed model for the spiral inductor

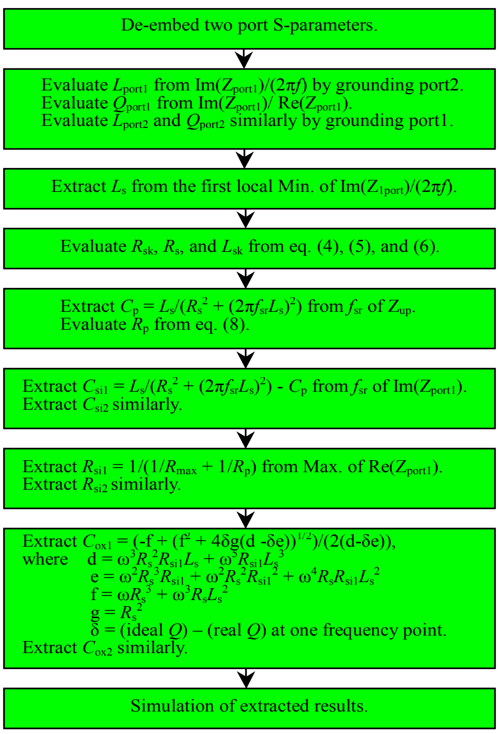

Fig. 2 The schematic flow chart of the extraction program.

Acknowledgements

The authors would like to thank the staff members of UMC for their helpful comments and great supports.

References

[1] W. B. Kuhn *et al.*, "Analysis of the current crowding effects in multiturn spiral inductors," IEEE J. Trans. Microwave Theory Tech., vol. 49, pp. 31-38, Jan. 2001.

[2] B. L. Ooi *et al.*, "An improved prediction of series resistance in spiral inductor modeling with eddy-current effect," IEEE Trans. Microwave Theory Tech., vol. 50, pp. 2202, Sep. 2002.

[3] Y. Cao *et al.*, "Frequency-independent equivalent-circuit model for on-chip spiral inductors," IEEE J. Solid-State Circuits, vol. 38, pp. 419-426, Mar. 2003.

[4] C. Y. Su *et al.*, "A macro model of silicon spiral inductor," Solid-State Electronics, vol. 46, pp. 759-767, May 2002.

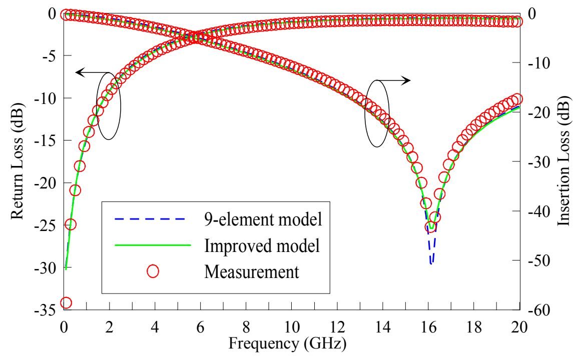

Fig. 3 Measured and simulated results of return loss and insertion loss of the spiral inductor

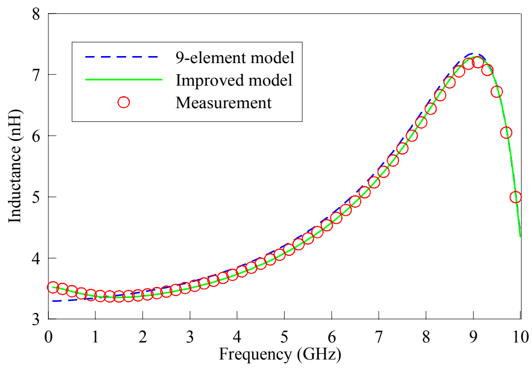

Fig. 4 Measured and simulated results of inductance for the inductor.

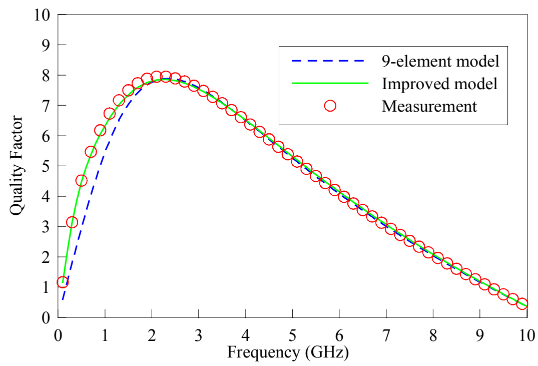

Fig. 5 Measured and simulated results of quality factor for the inductor.